Cd(II) complexes of 9-anthracenyl-4'-benzoate and 4-pyridyl vinyl arenes: effect of steric hindrance in the solid-state photoreactivity

K. Mohamed Yusuf Baig and Goutam Kumar Kole*

Department of Chemistry, College of Engineering and Technology, SRM Institute of Science and Technology, Kattankulathur, Tamil Nadu 603203, India.

Emails: goutamks@srmist.edu.in

Table of contents

1. Crystallographic data

Table S1. Crystallographic data for ligand and complexes **1** – **4**

Compd.	**9-AnBzH·DMF**	**1**	**2**
CCDC No.	2394023	2394024	2394025
Formula	$C_{24}H_{21}NO_3$	$C_{70}H_{56}CdN_2O_7$	$C_{154}H_{112}Cd_2N_4O_{10}$
Formula weight ($g.mol^{-1}$)	371.42	1149.58	2403.30
Temperature (K)	298(2)	298(2)	298(2)
Radiation, λ (Å)	Mo Kα (λ = 0.71073)	Mo Kα (λ = 0.71073)	Mo Kα (λ = 0.71073)
Crystal Colour, habit	Colourless, Block	Colourless, Block	Yellow, Block
Crystal size (mm^3)	0.380 x 0.250 x 0.190	0.270 x 0.130 x 0.100	0.256 x 0.122 x 0.119
Crystal system	Monoclinic	Triclinic	Triclinic
Space Group	$P2_1/c$	$P\bar{1}$	$P\bar{1}$
Unit cell dimensions			
a (Å)	15.5236(5)	7.2804(5)	14.4148(4)
b (Å)	7.6804(2)	13.7782(10)	15.8764(5)
c (Å)	18.3531(5)	15.2825(11)	16.3965(5)
α (º)	90	106.655(2)	61.050(2)
β (º)	114.761(1)	92.239(2)	75.044(3)
γ (º)	90	103.923(2)	63.886(5)
Volume ($Å^3$)	1987.02(10)	1415.88(18)	2943.5(2)
Z	4	1	1
Calculated density ($Mg.m^{-3}$)	1.242	1.351	1.356
μ (mm^{-1})	0.082	0.444	0.428
θ range (°)	2.259 to 26.368	2.426 to 26.020	2.182 to 26.371
Reflections collected	19957	38719	112254
Independent reflections	4051	5533	12026
Parameters/ restraints	297/20	369/6	771/0
GooF on F^2	1.058	1.123	1.110
R_1 [I>2σ(I)]	0.0463 (3176)	0.0842 (5341)	0.0317 (10281)
wR_2 (all data)	0.1343 (4051)	0.2528 (5533)	0.0903 (12026)
Maximum/minimum residual electron density ($e.Å^{-3}$)	0.153/-0.146	5.299/-0.782	0.619/-0.511

Compd.	**3**	**4**
CCDC No.	2394026	2394027
Formula	$C_{152}H_{104}Cd_2N_4O_8$	$C_{86}H_{64}CdN_2O_6$
Formula weight (g.mol^{-1})	2339.22	1333.80
Temperature (K)	298(2)	295(2)
Radiation, λ (Å)	Mo Kα (λ = 0.71073)	Mo Kα (λ = 0.71073)
Crystal Colour, habit	Colourless, Block	Yellow, Block
Crystal size (mm^3)	0.230 x 120 x 100	0.330 x 0.190 x 0.110
Crystal system	Monoclinic	Monoclinic
Space Group	*C*2/*c*	$P2_1/n$
Unit cell dimensions		
a (Å)	20.408(6)	15.144(4)
b (Å)	27.538(9)	14.803(5)
c (Å)	22.646(4)	15.759(4)
α (º)	90	90
β (º)	112.654(8)	109.241(11)
γ (º)	90	90
Volume (Å^3)	11745(6)	3335.5(17)
Z	4	2
Calculated density (Mg.m^{-3})	1.323	1.328
μ (mm^{-1})	0.426	0.386
θ range (°)	2.163 to 26.372	1.941 to 26.370
Reflections collected	119334	48177
Independent reflections	12013	6818
Parameters/ restraints	767/44	435/1
GooF on F^2	1.080	1.094
R_1 [I>2σ(I)]	0.0395 (9907)	0.0372 (5673)
wR_2 (all data)	0.0943 (12013)	0.1027 (6818)
Maximum/minimum residual electron density (e.Å^{-3})	0.444/-0.269	1.049/-0.275

2. Additional structural diagrams

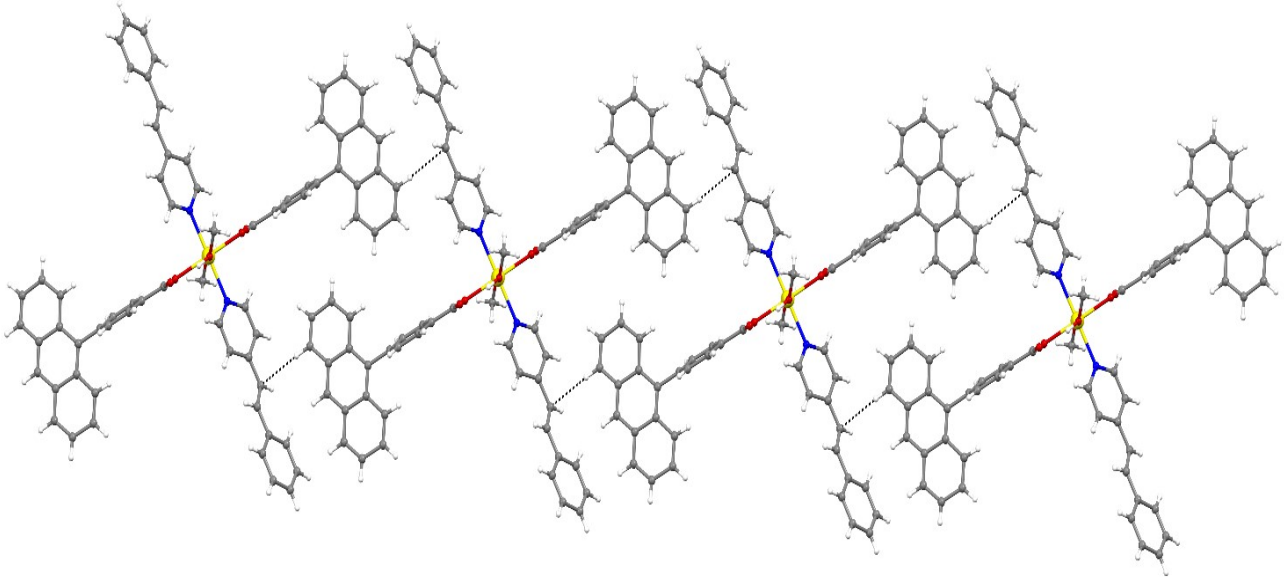

Fig. S1. Crystal packing of **1** showing C−H···π weak interactions, viewed approximately along the *a*-direction**.**

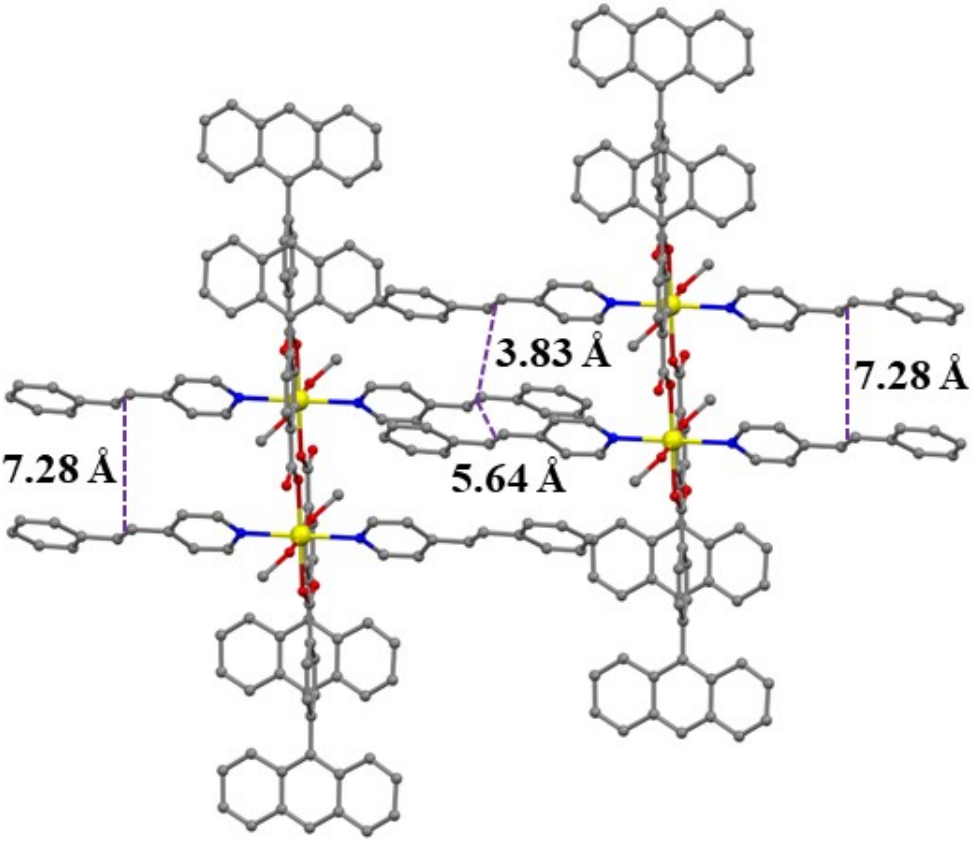

Fig. S2. The observed *head-to-tail* alignment of **4-StPy** is suitable for [2 + 2] photocycloaddition reaction in **1**, where the *head-to-head* alignment of **4-StPy** is unsuitable. Hydrogen atoms are omitted for clarity.

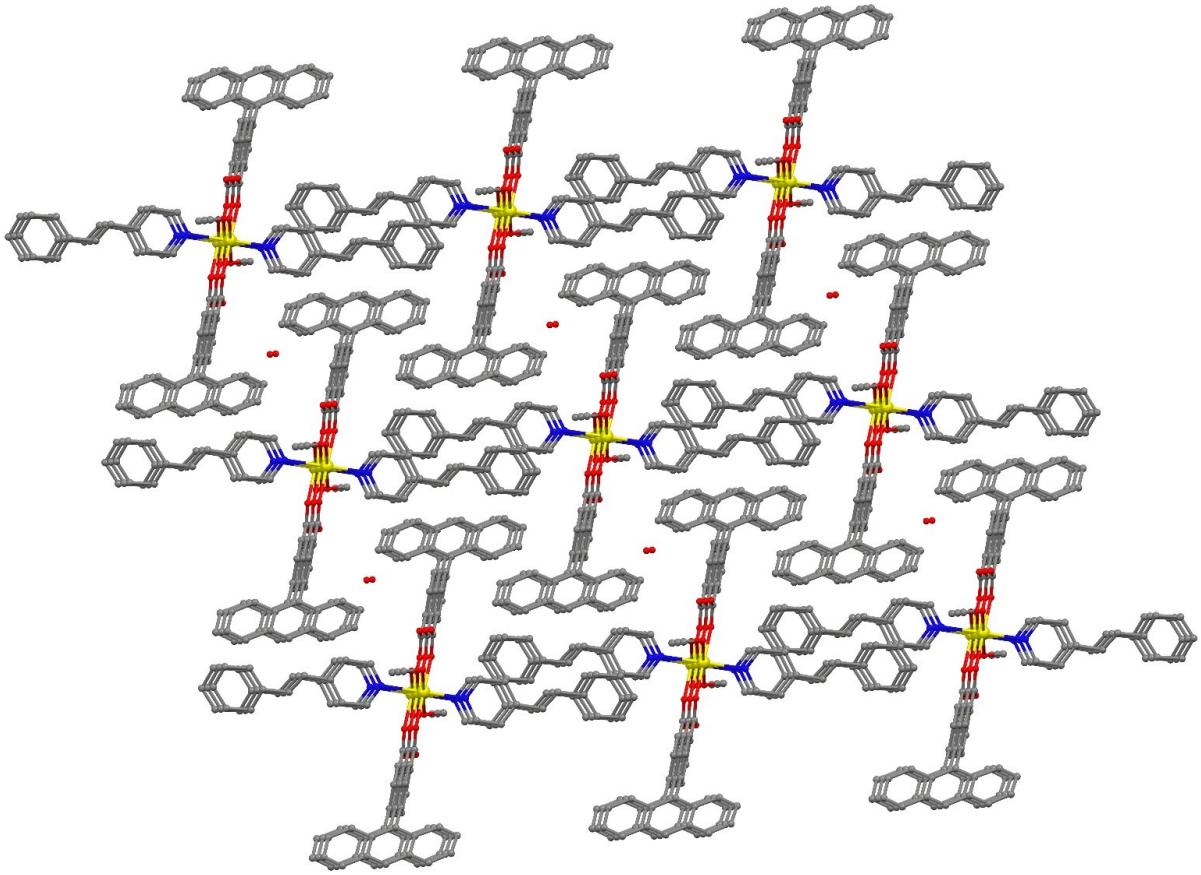

Fig. S3. Packing of **1** viewed along the *a*-direction.

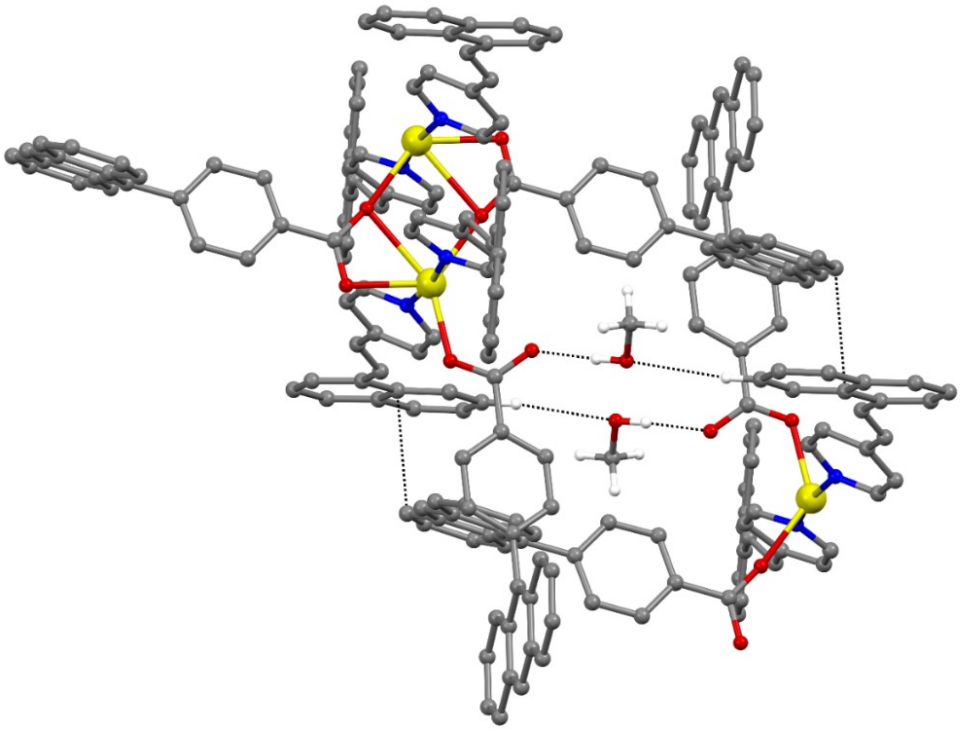

Fig. S4. The intermolecular interactions of C−H···π, O−H···O and π···π interactions observed in **2**. Only selected hydrogen atoms are shown for clarity.

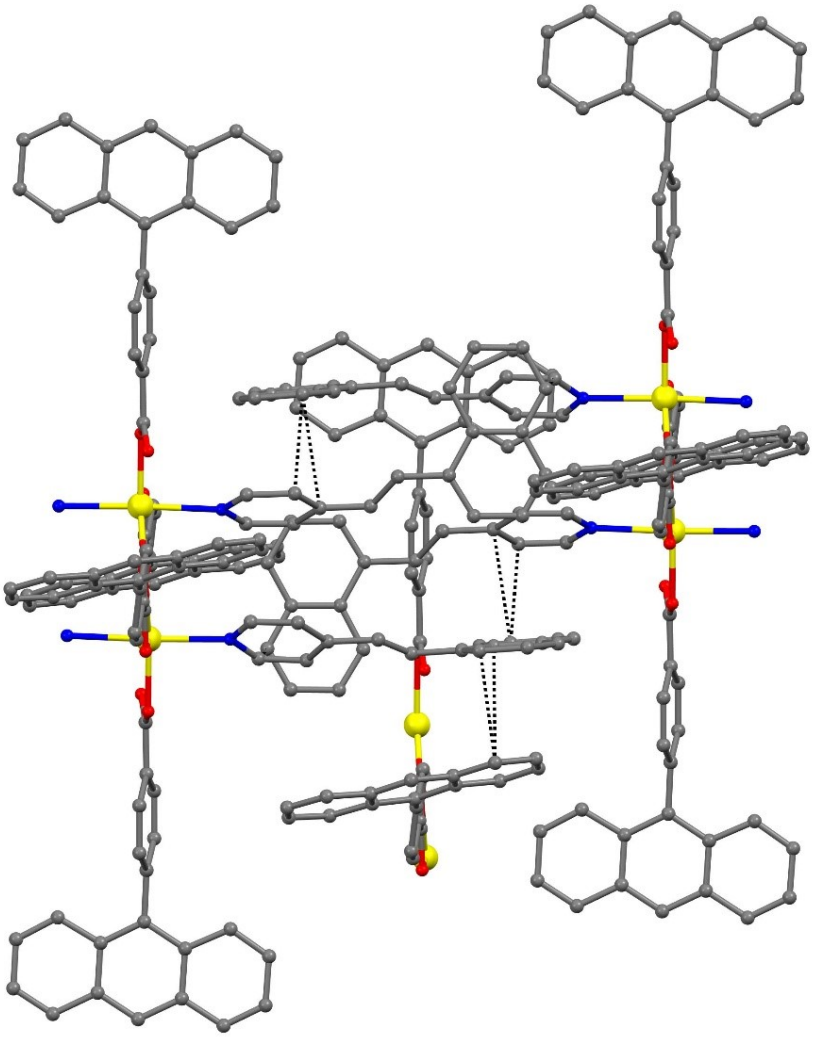

Fig. S5. The π···π interactions between the observed between naphthalene moieties, and between naphthalene and anthracene moieties in **2**. Hydrogen atoms are omitted for clarity.

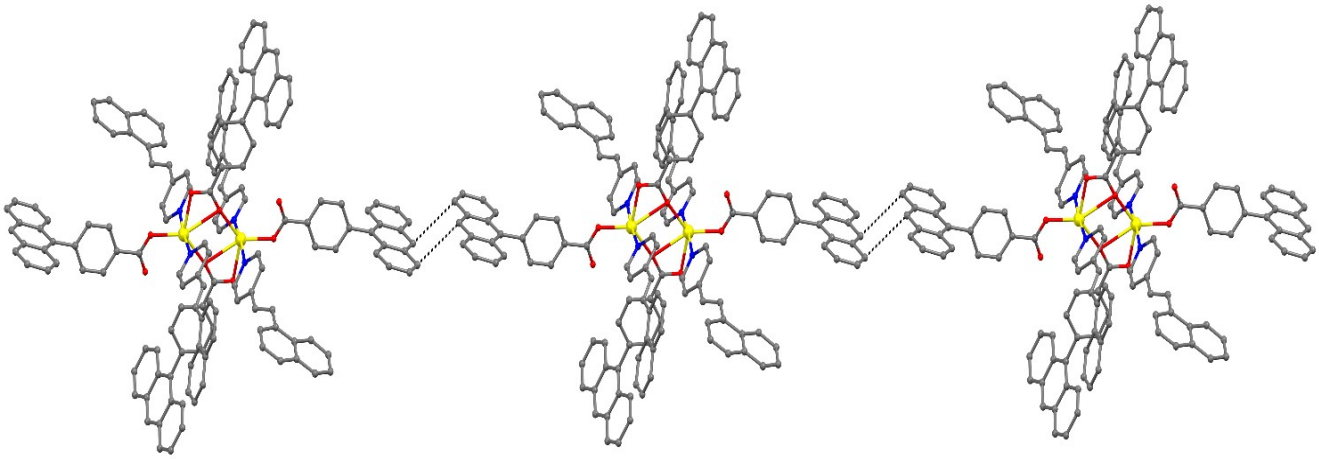

Fig. S6. The π···π interactions between the two different **9-AnBz** moieties in **2**. Hydrogen atoms are omitted for clarity.

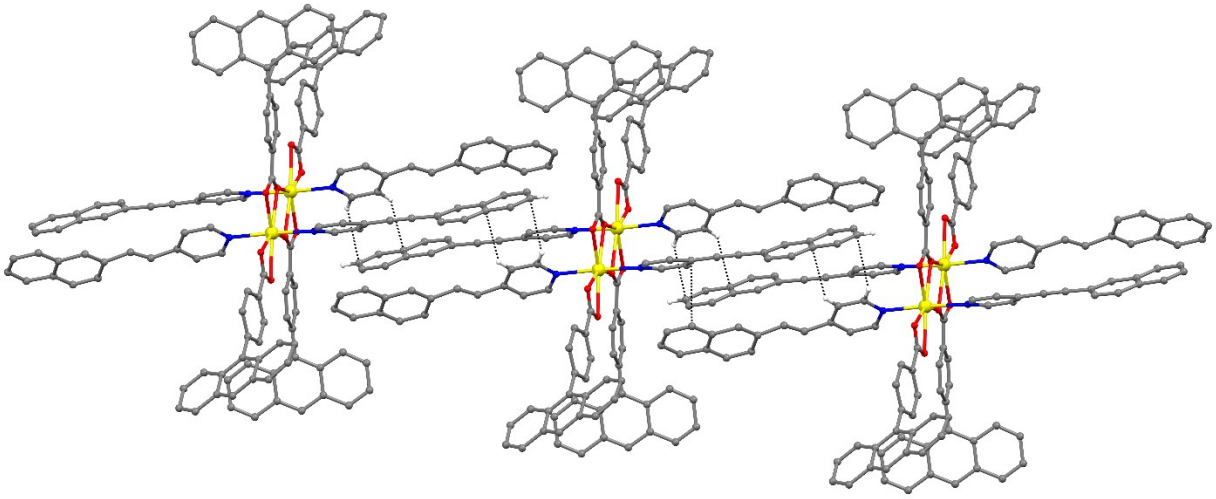

Fig. S7. Two neighbouring complexes of **2-NVP** ligands form C−H···π interactions with pyridyl C−H bonds and naphthalene moieties in **3**. Only selected hydrogen atoms are shown for clarity.

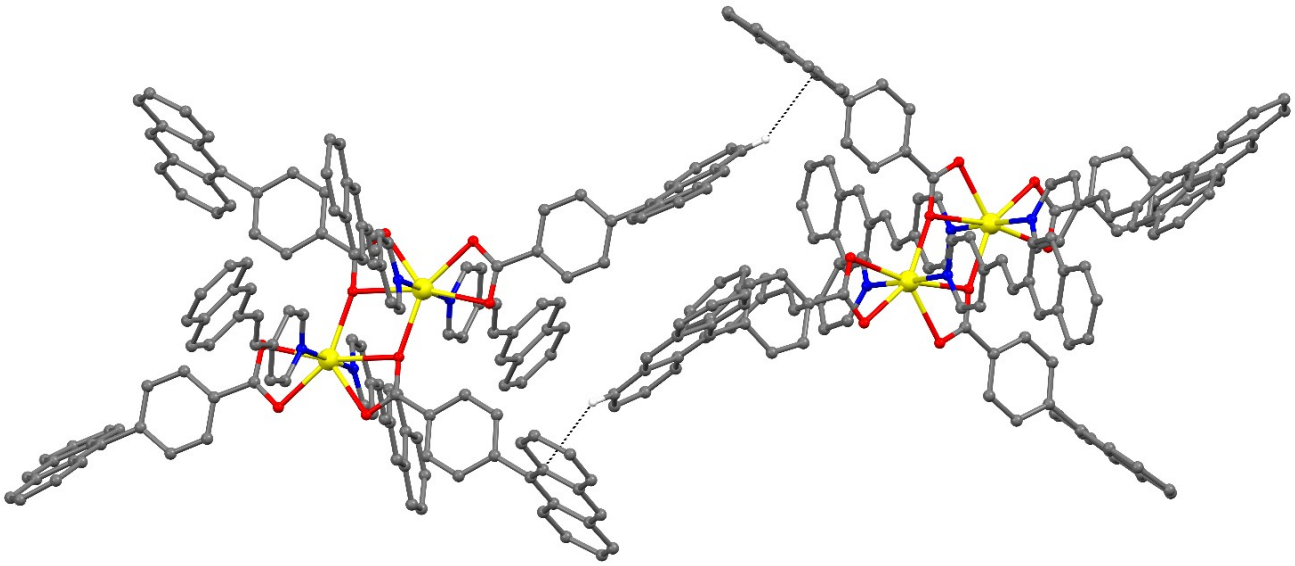

Fig. S8. The C−H···π interactions between the two different **9-AnBz** moieties in **3**. Only selected hydrogen atoms are shown for clarity.

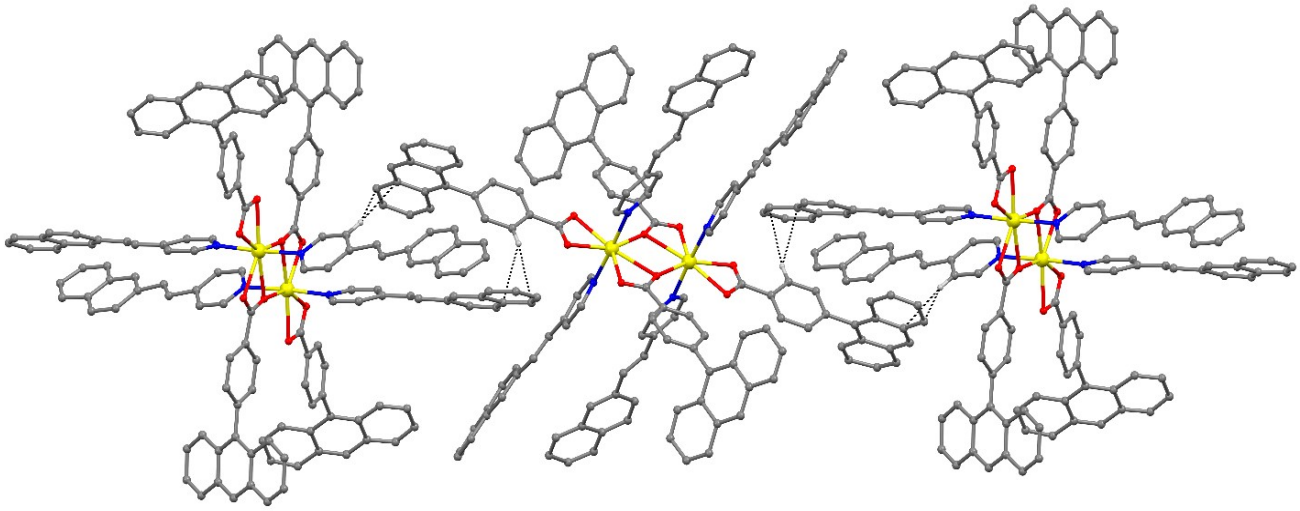

Fig. S9. The C−H···π interactions between the **9-AnBz** and **2-NVP** ring in **3** were observed**.** Only selected hydrogen atoms are shown for clarity.

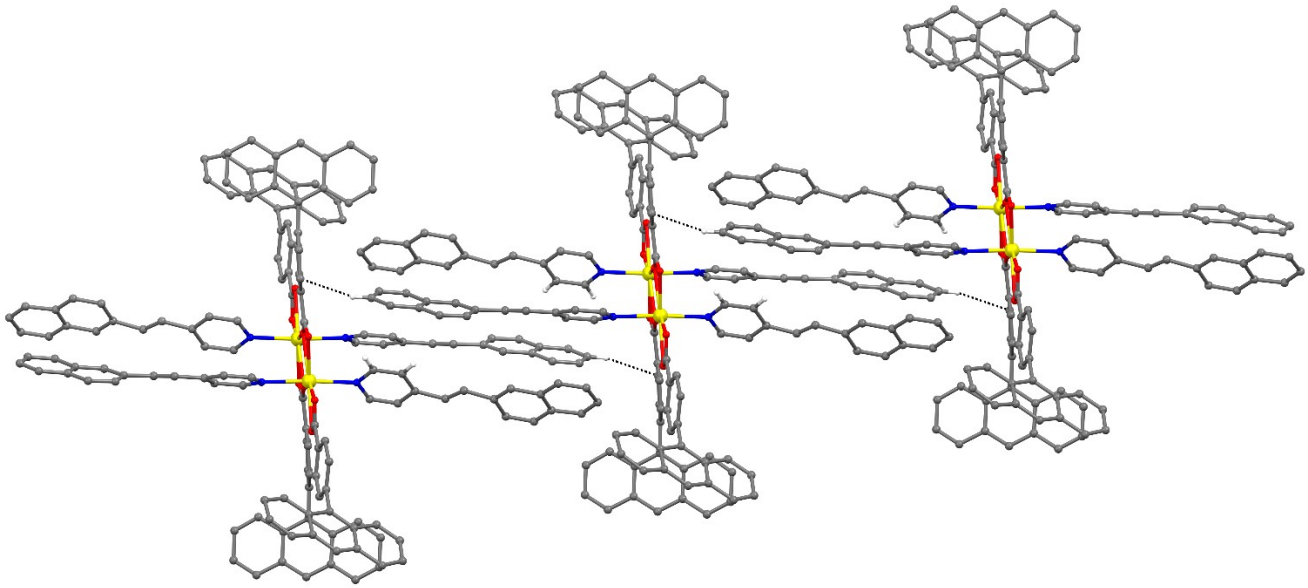

Fig. S10. Additional C−H···π interactions in **3.** Only selected hydrogen atoms are shown for clarity.

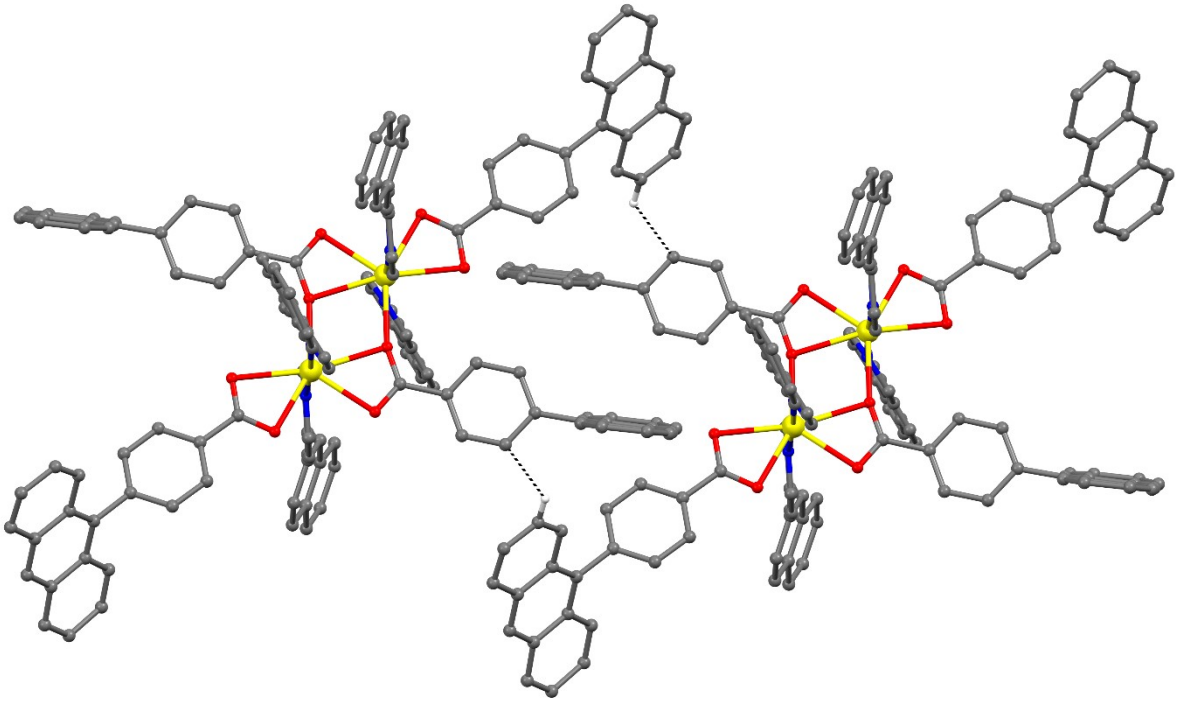

Fig. S11. Anthracene moieties exert C−H···π interactions separately with the phenyl C−H bonds of other **9-AnBz** ligands in **3**. Only selected hydrogen atoms are shown for clarity.

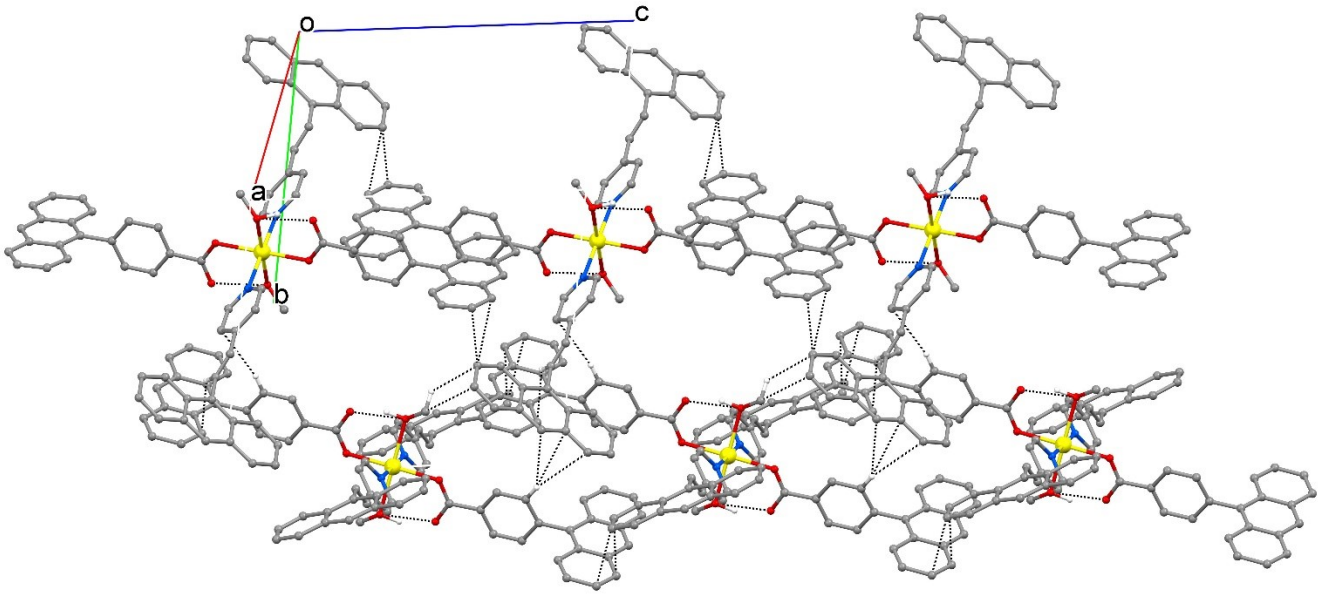

Fig. S12. The C−H···π, O−H···O, and π···π interactions present in the crystal packing of **4.** Only selected hydrogen atoms are shown for clarity.

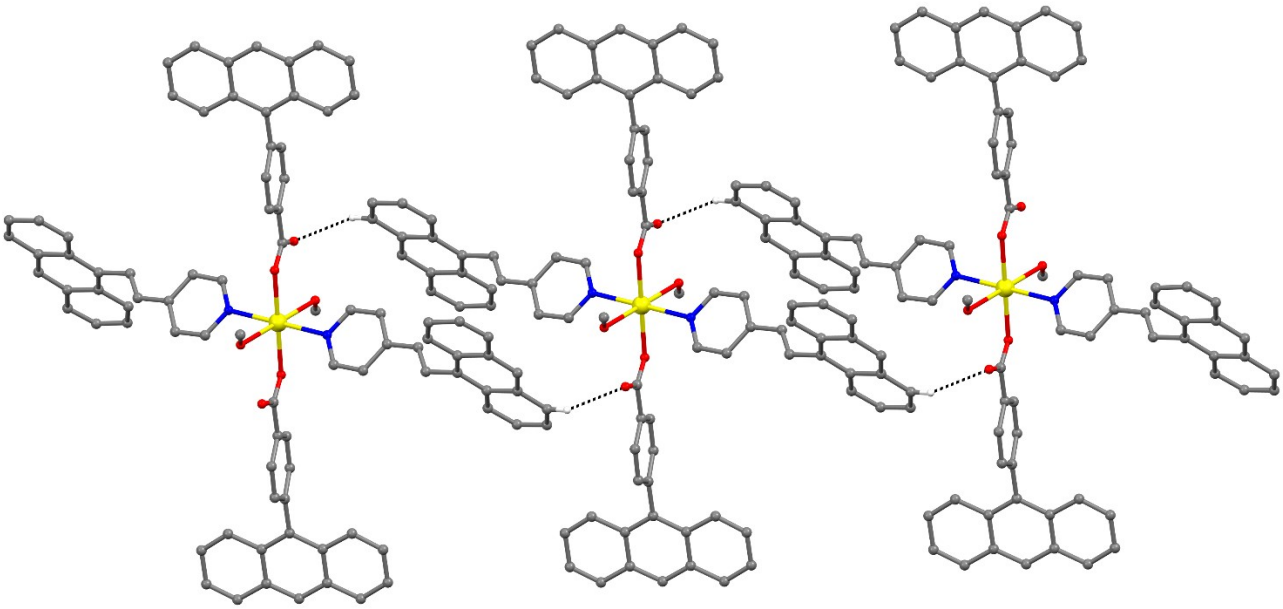

Fig. S13. The C−H···O interaction was observed between the anthracene C−H bonds and carboxyl-O of **9-AnBz** in **4.** Only selected hydrogen atoms are shown for clarity.

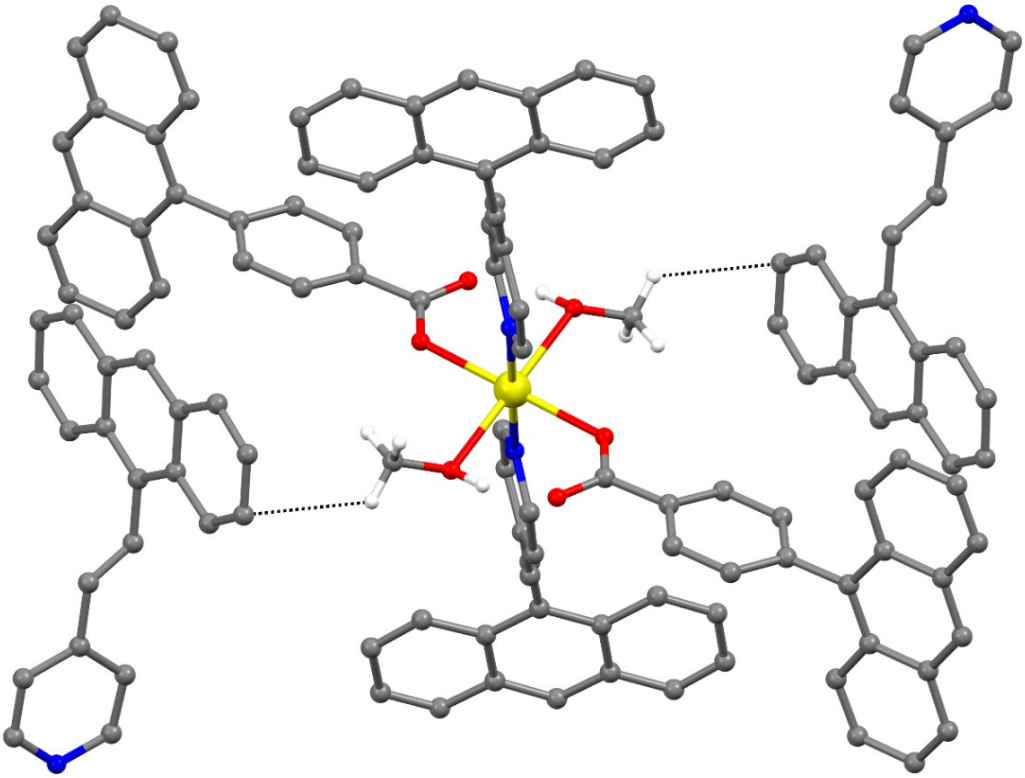

Fig. S14. Additional C−H···π interaction between the methanol and anthracene moiety in **4.** Only selected hydrogen atoms are shown for clarity.

3. Powder X-ray diffraction

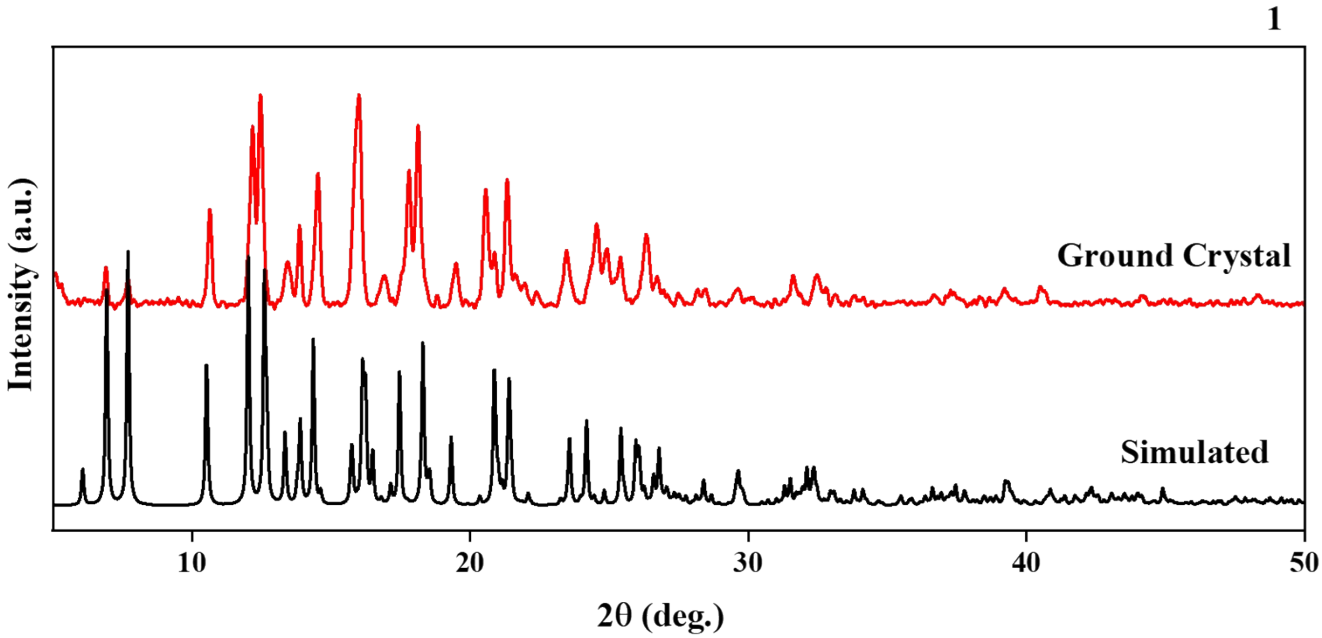

Fig. S15. Simulated PXRD pattern of **1** agrees with the experimentally observed pattern.

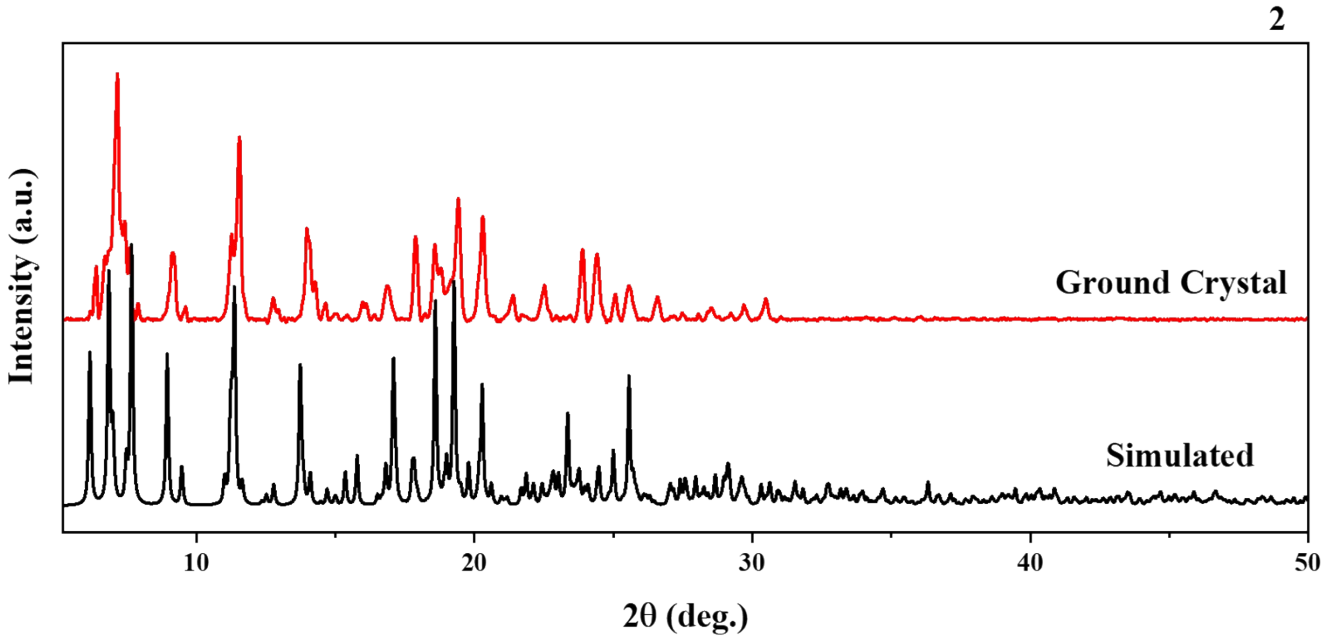

Fig. S16. Comparison of the simulated and observed PXRD patterns of **2.**

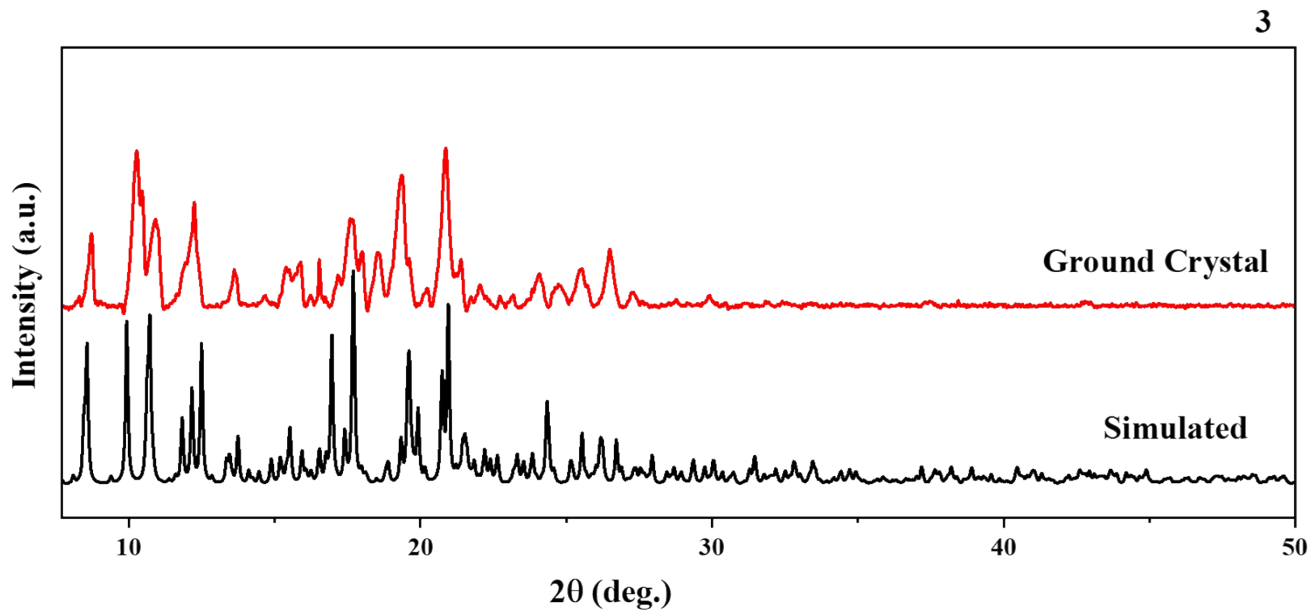

Fig. S17. Simulated PXRD pattern of **3** matches with the experimentally observed pattern**.**

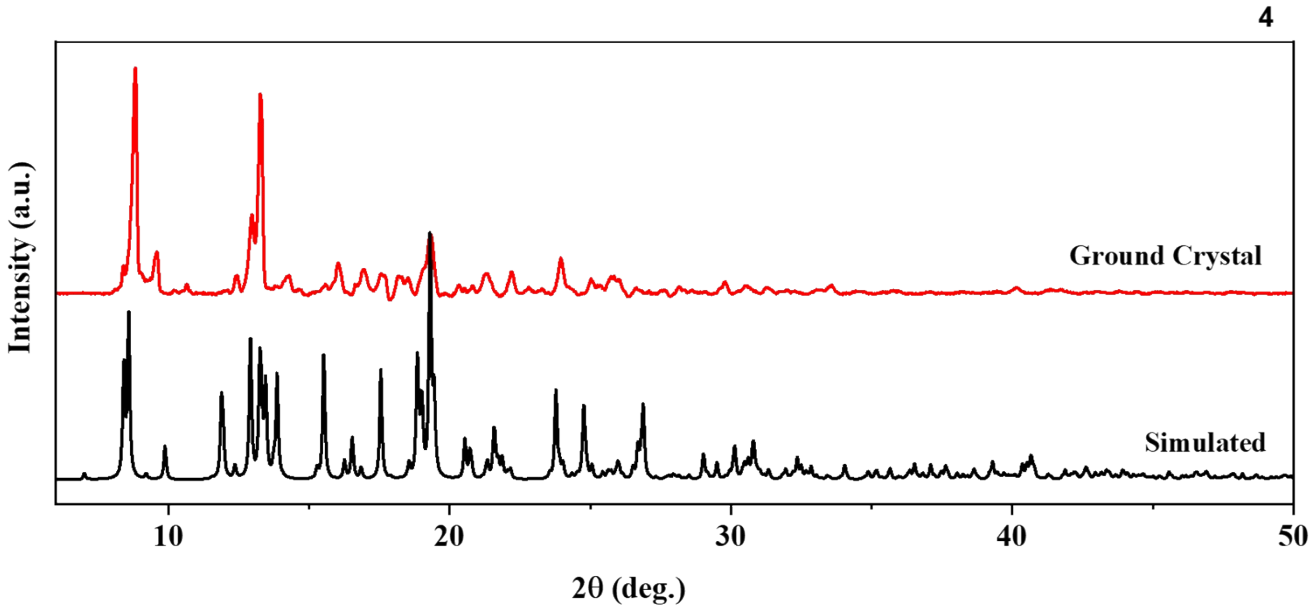

Fig. S18. Simulated and experimentally observed PXRD patterns of **4**. Their disagreement suggests the presence of a mixture of compounds**.**

4. Solid state UV-Vis absorption (DRS)

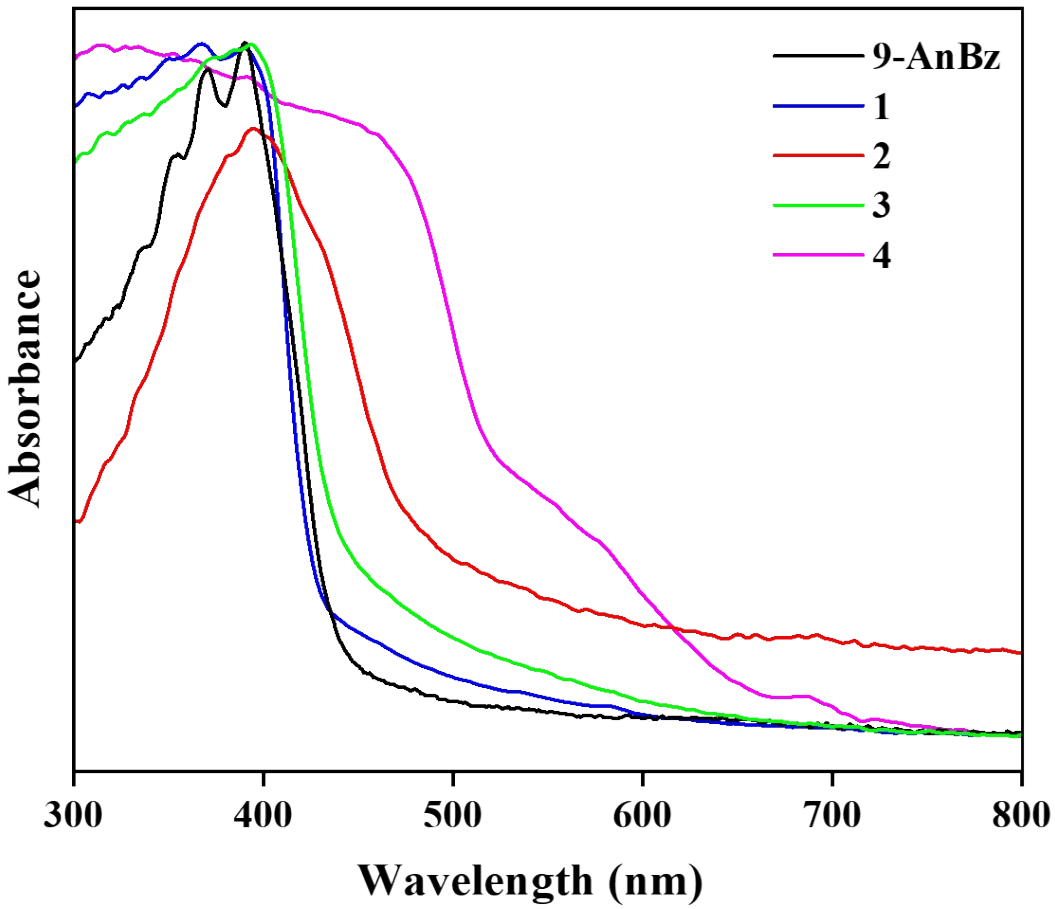

Fig. S19. Solid-state absorption (DRS) spectra of **1** – **4**.

5. NMR spectroscopy

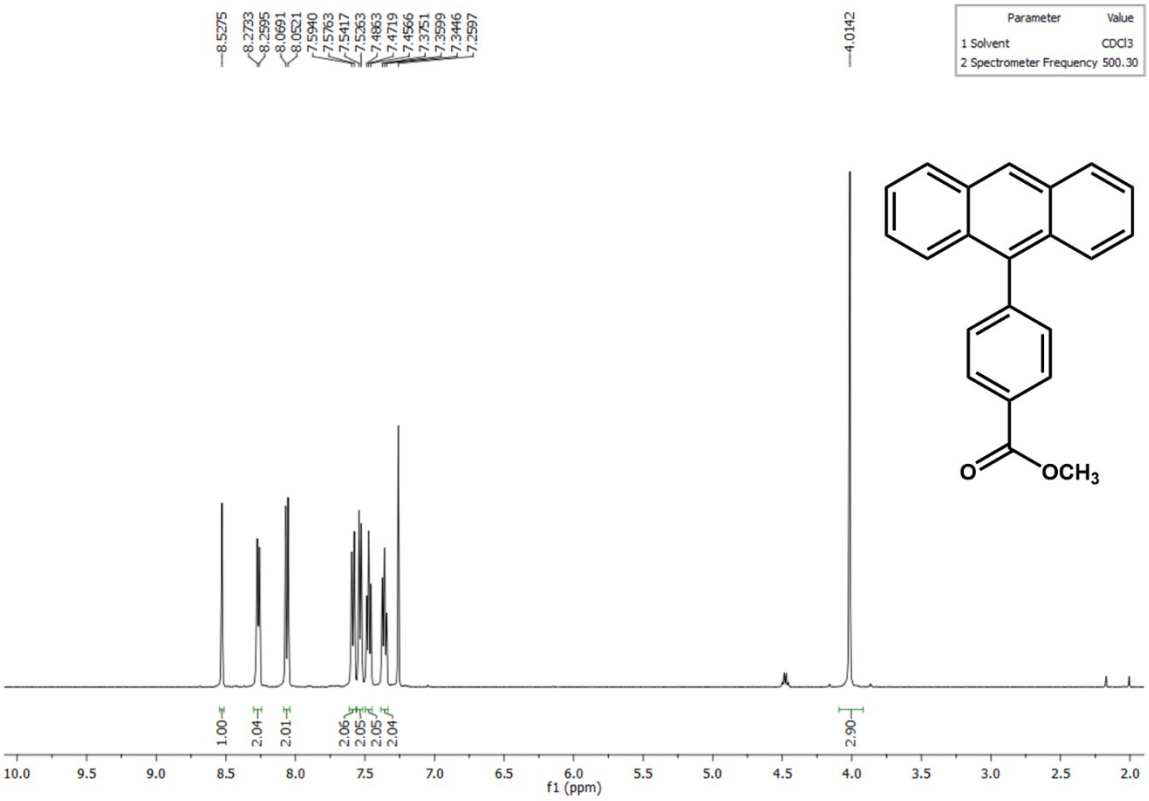

Fig. S20. ^{1}H NMR (500 MHz, $CDCl_3$) spectrum of **9-AnBzMe.**

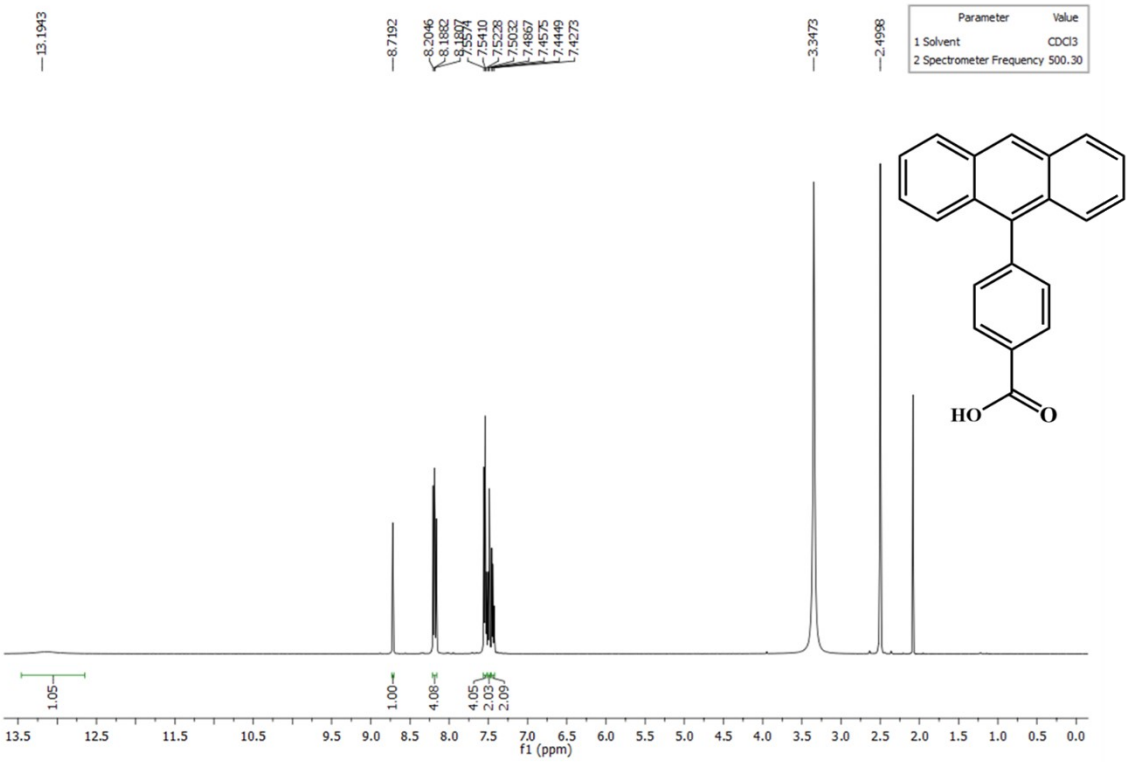

Fig. S21. ^{1}H NMR (500 MHz, DMSO-d_6) spectrum of **9-AnBzH**.

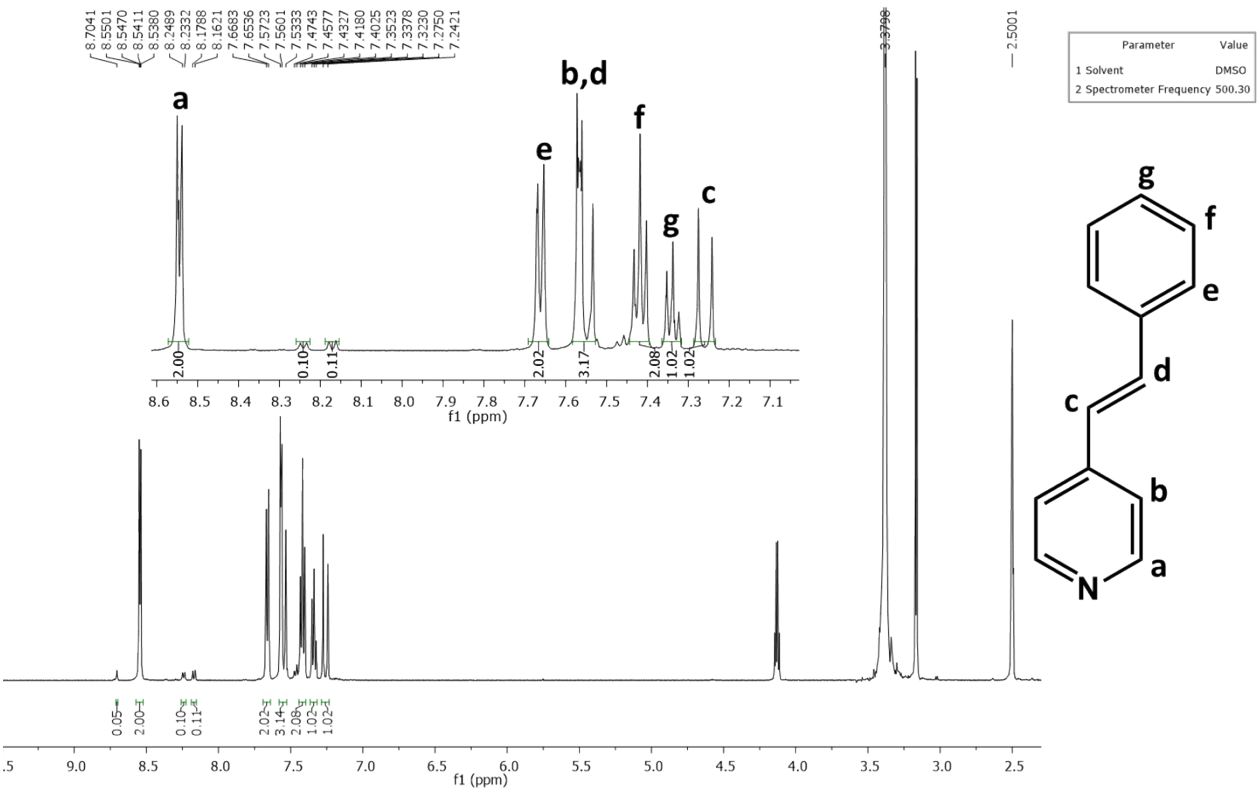

Fig. S22. ^{1}H NMR (500 MHz, DMSO-d_6) spectrum of **1**.

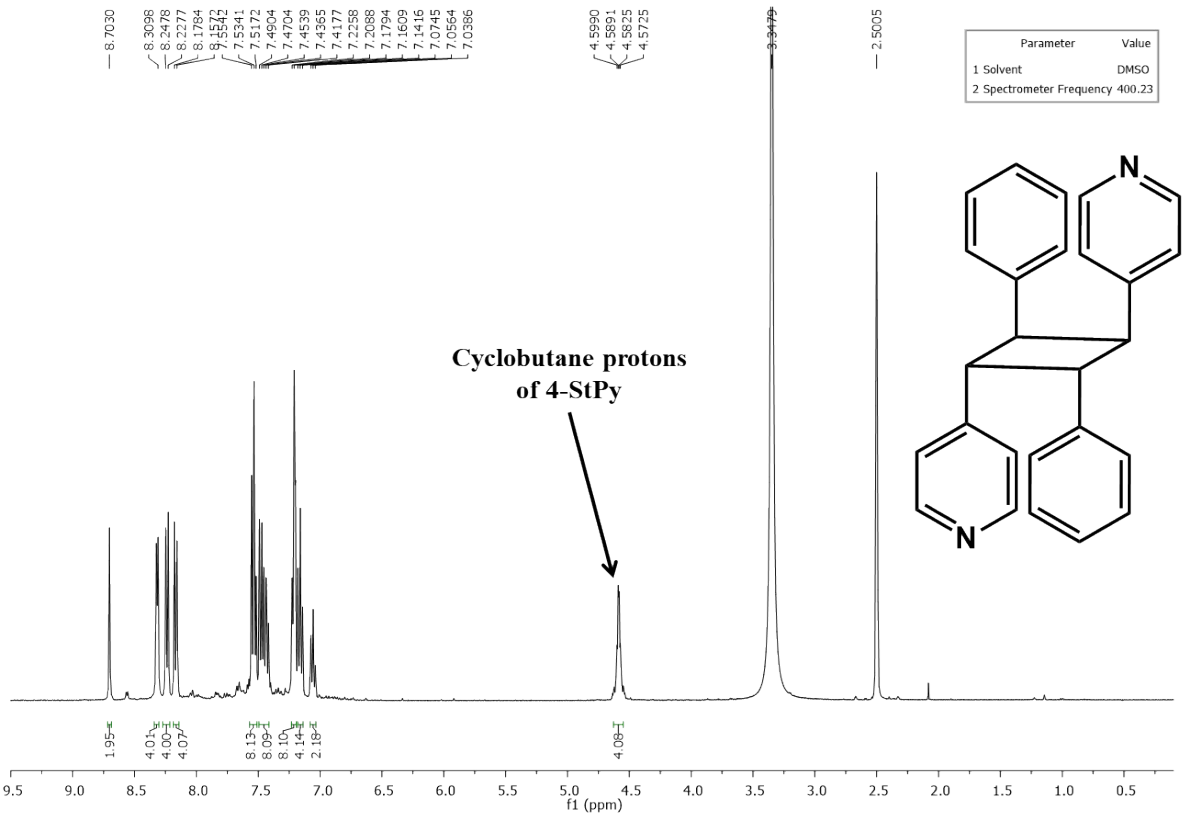

Fig. S23. ^{1}H NMR (400 MHz, DMSO-d_6) spectrum of **1** after exposure to sunlight for a few days suggests the photodimerization of **4-StPy** ligand.

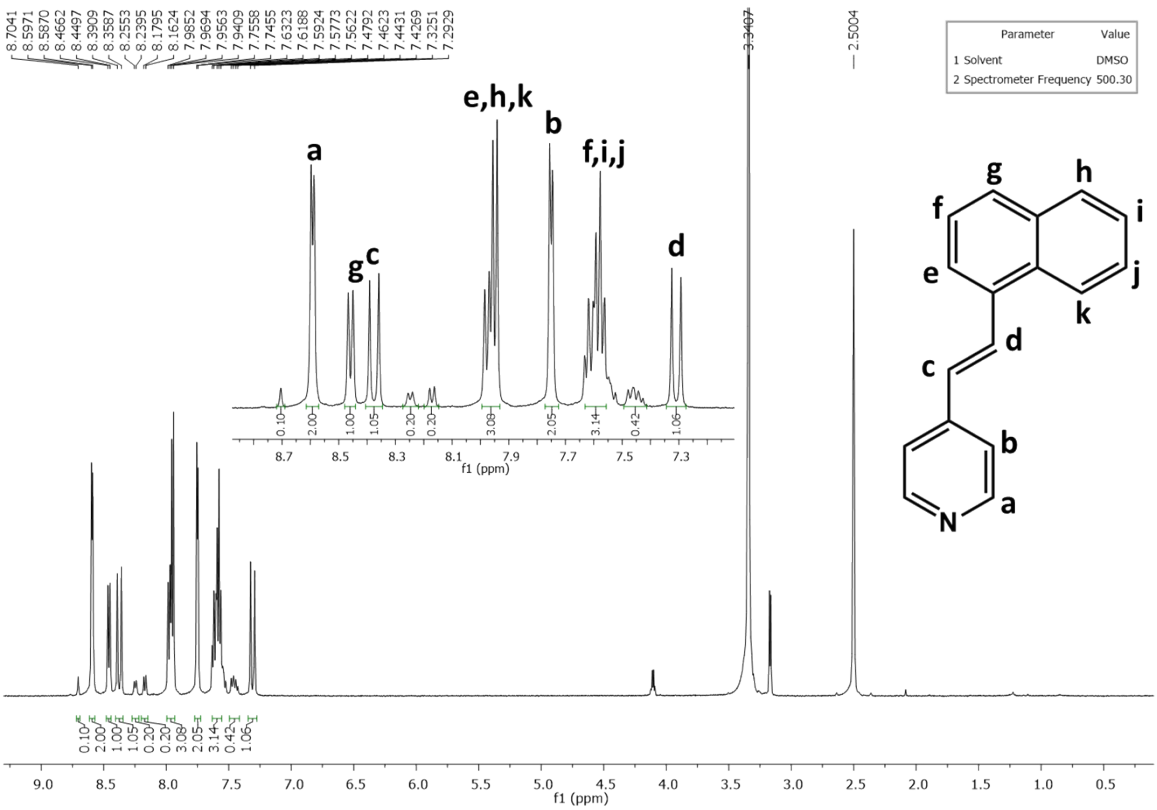

Fig. S24. ^{1}H NMR (500 MHz, DMSO-d_6) spectrum of **2**.

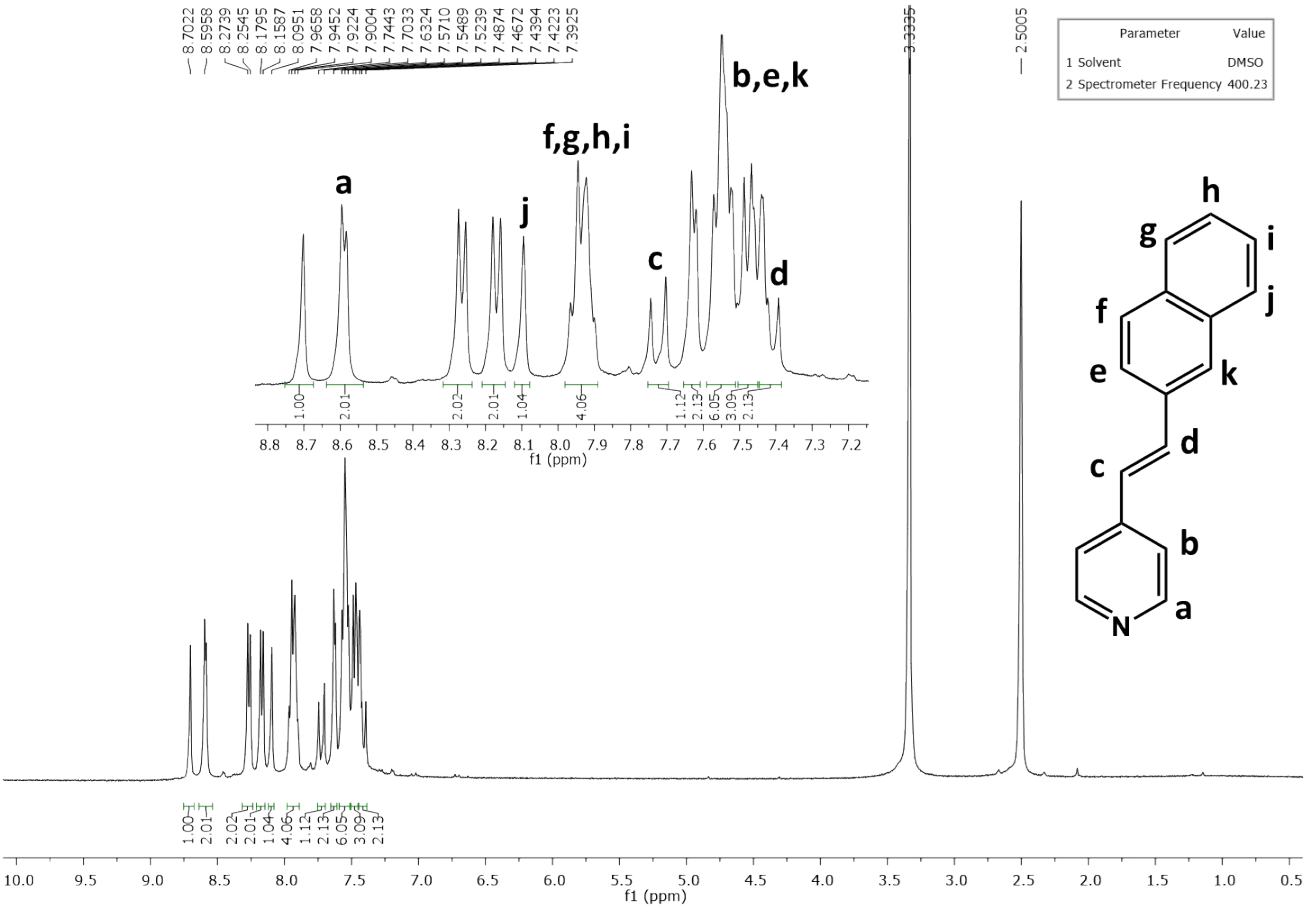

Fig. S25. ^{1}H NMR (400 MHz, DMSO-d_6) spectrum of **3**.

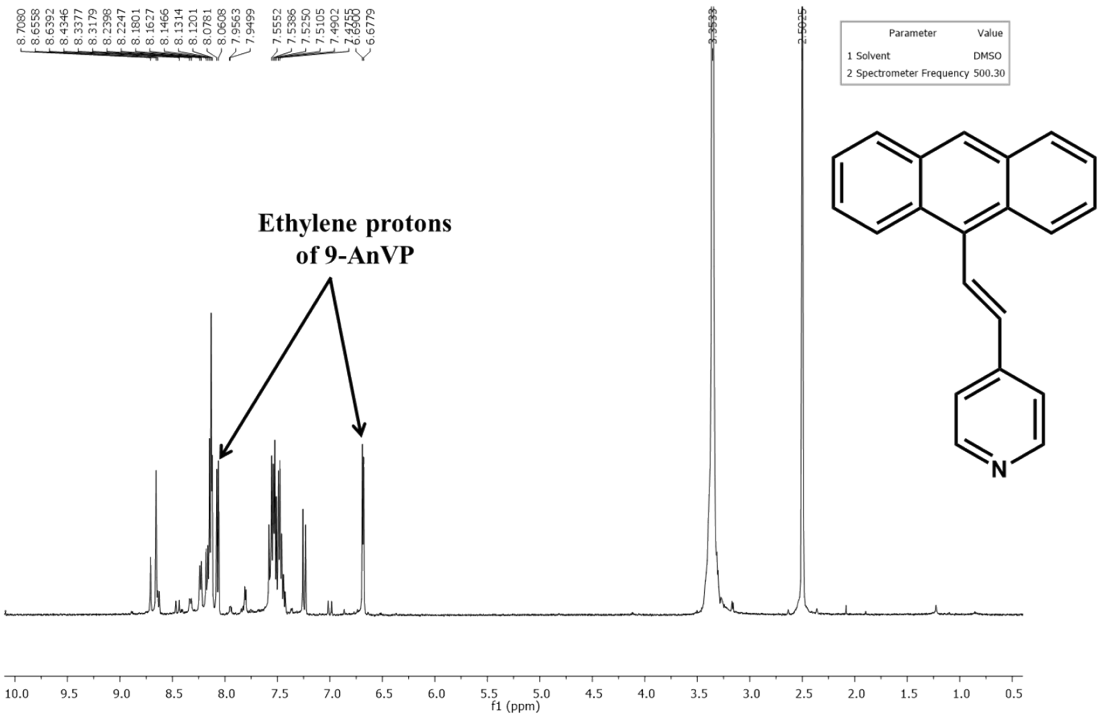

Fig. S26. ^{1}H NMR (500 MHz, DMSO-d_6) spectrum of **4**.

6. Thermogravimetric analysis

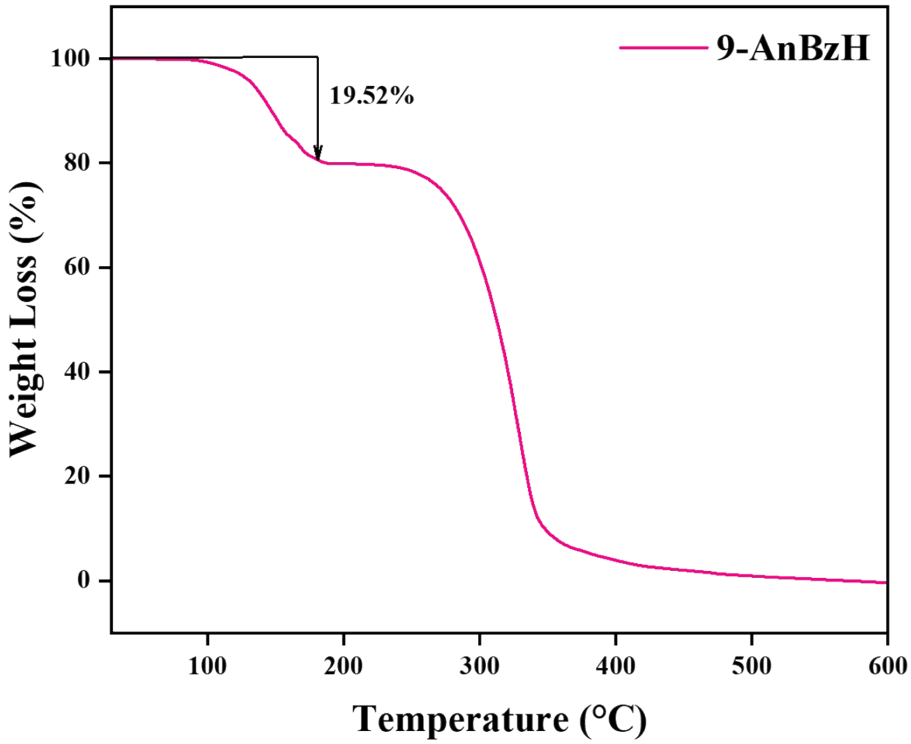

Fig. S27. TGA plot of **9-AnBzH·DMF**

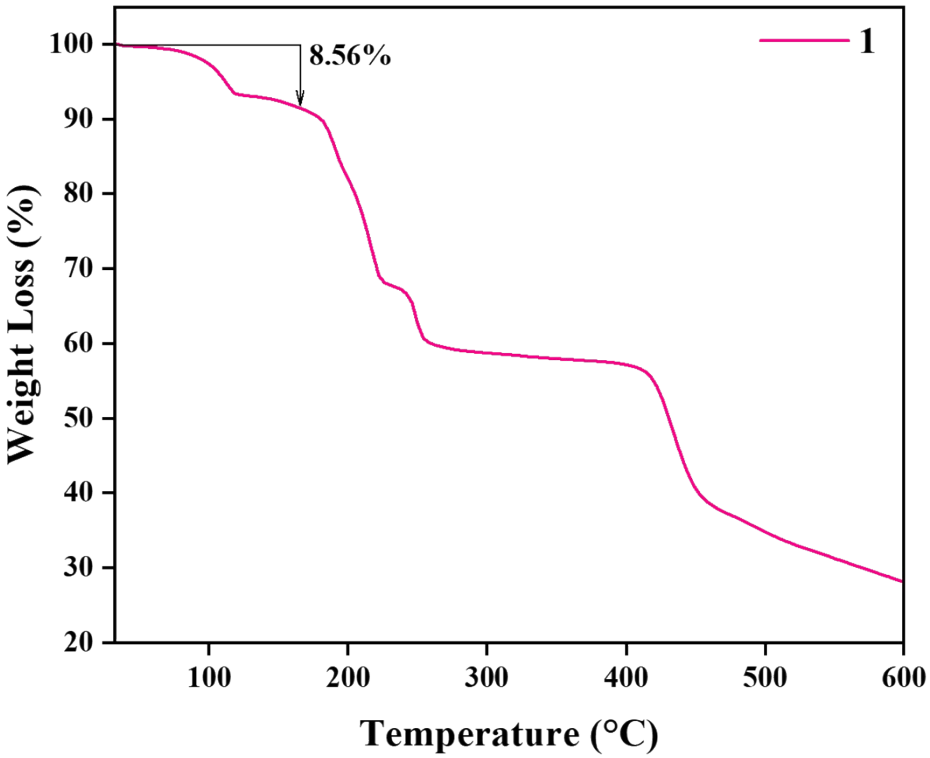

Fig. S28. TGA plot of **1.**

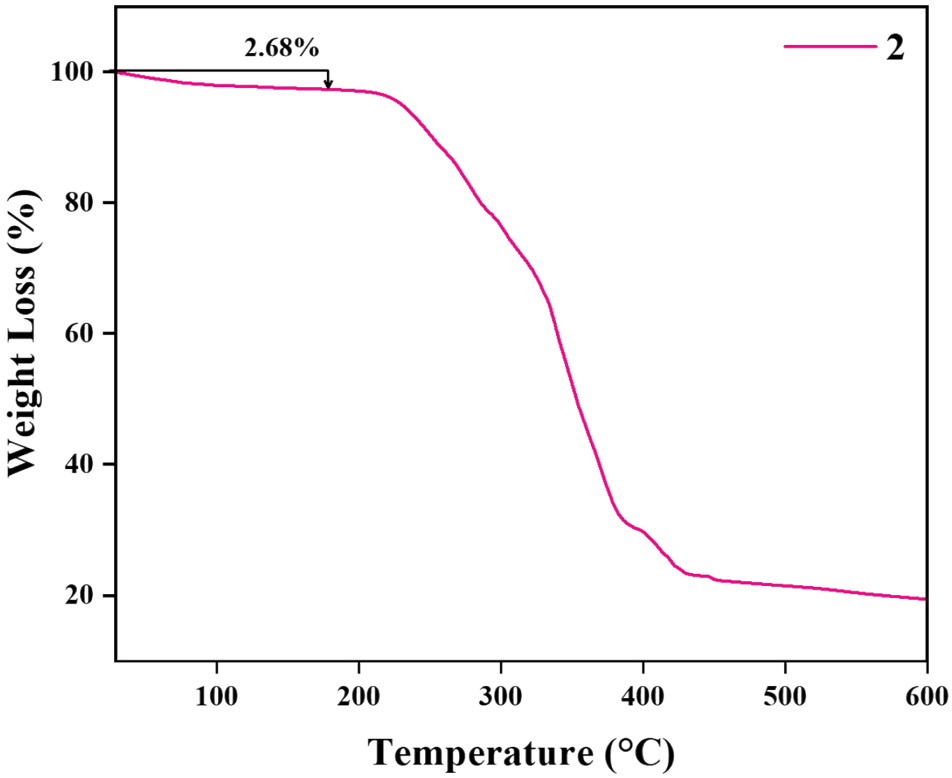

Fig. S29. TGA plot of **2**.

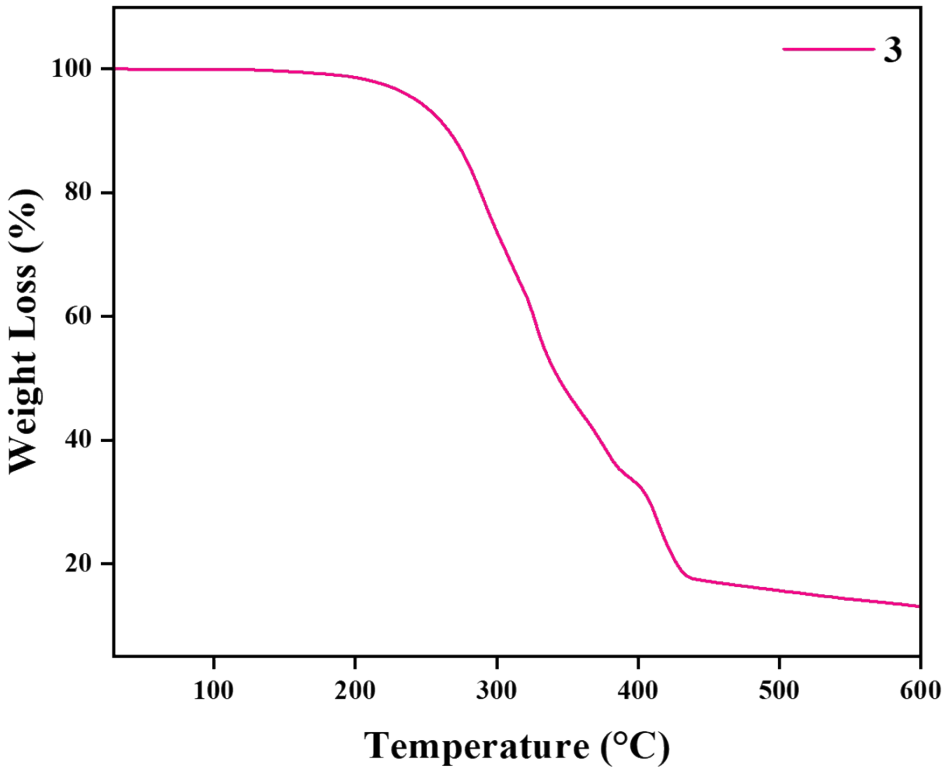

Fig. S30. TGA plot of **3**.

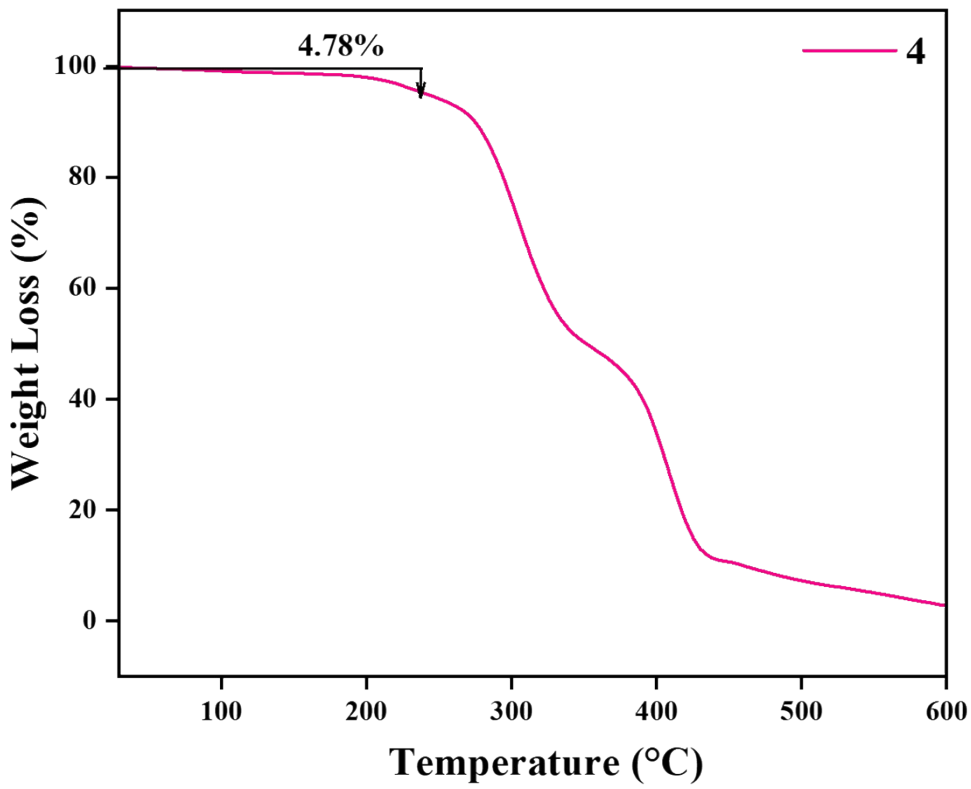

Fig. S31. TGA plot of **4**.

7. FT-IR spectroscopy

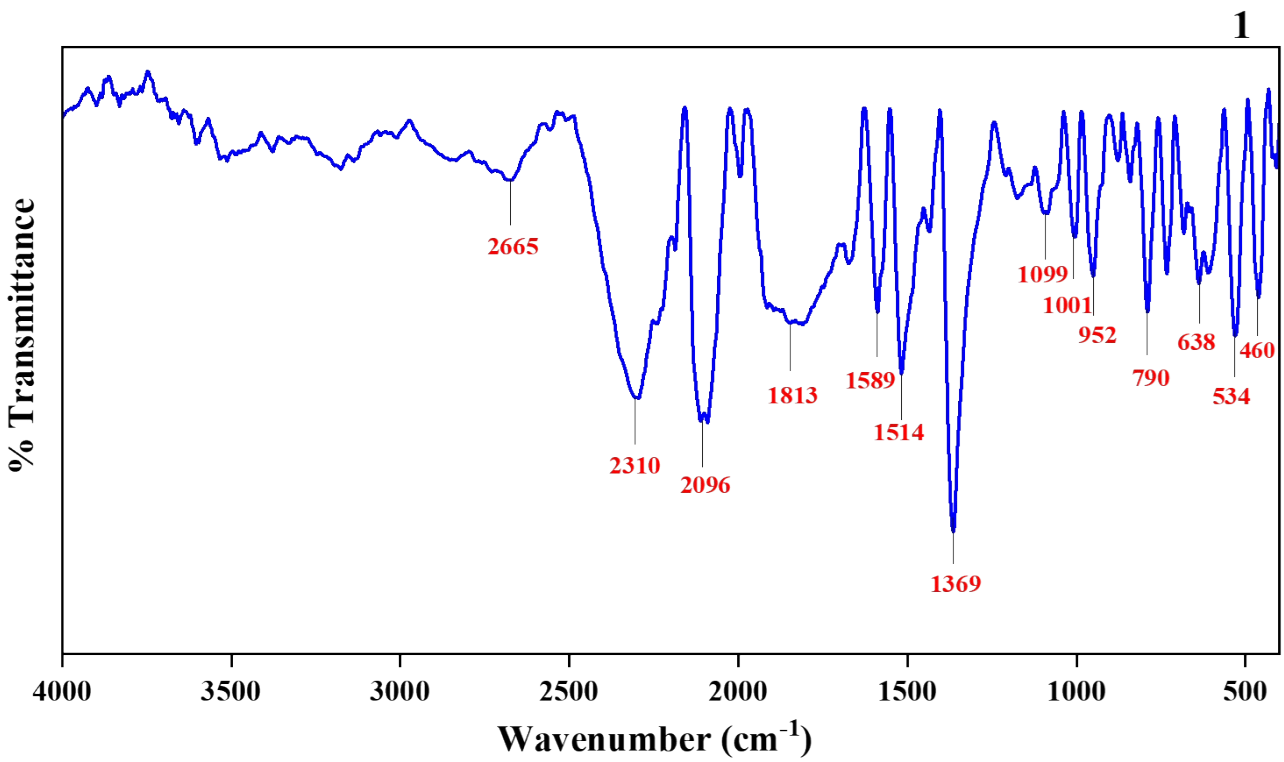

Fig. S32. FT-IR (KBr, cm^{-1}) spectrum of **1**.

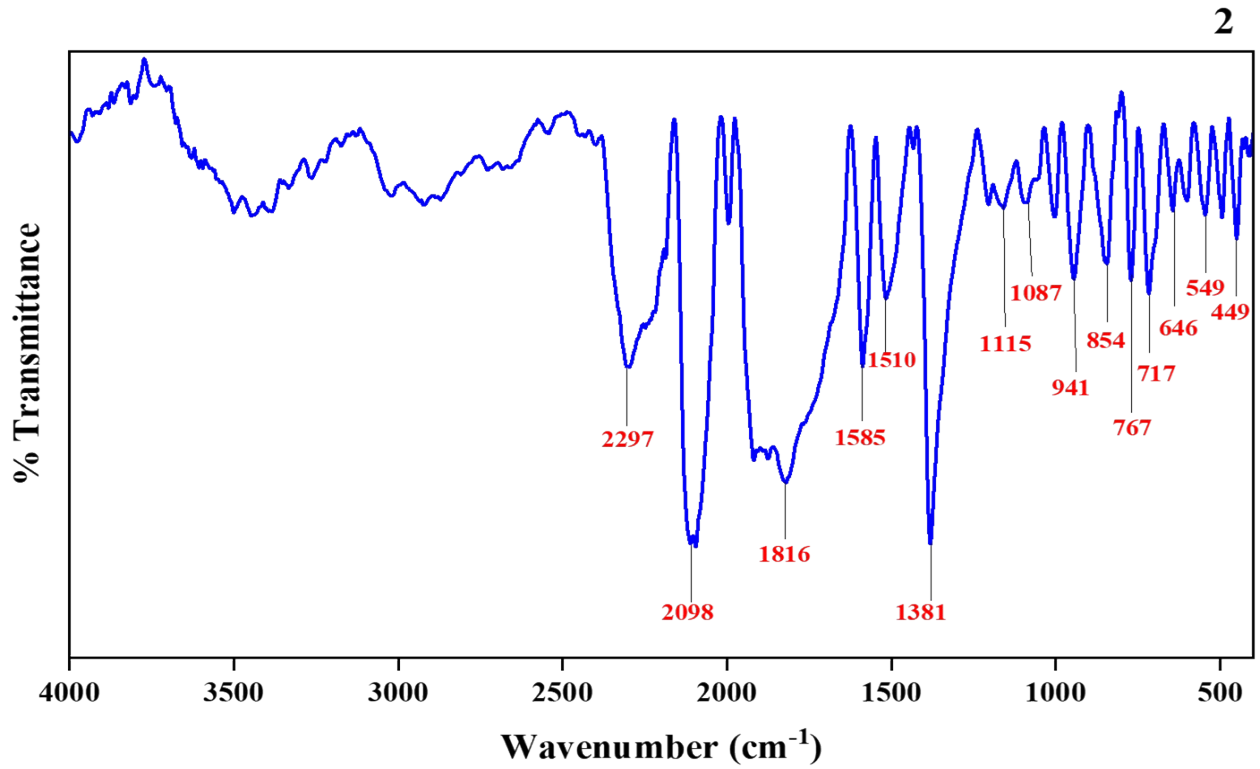

Fig. S33. FT-IR (KBr, cm^{-1}) spectrum of **2**.

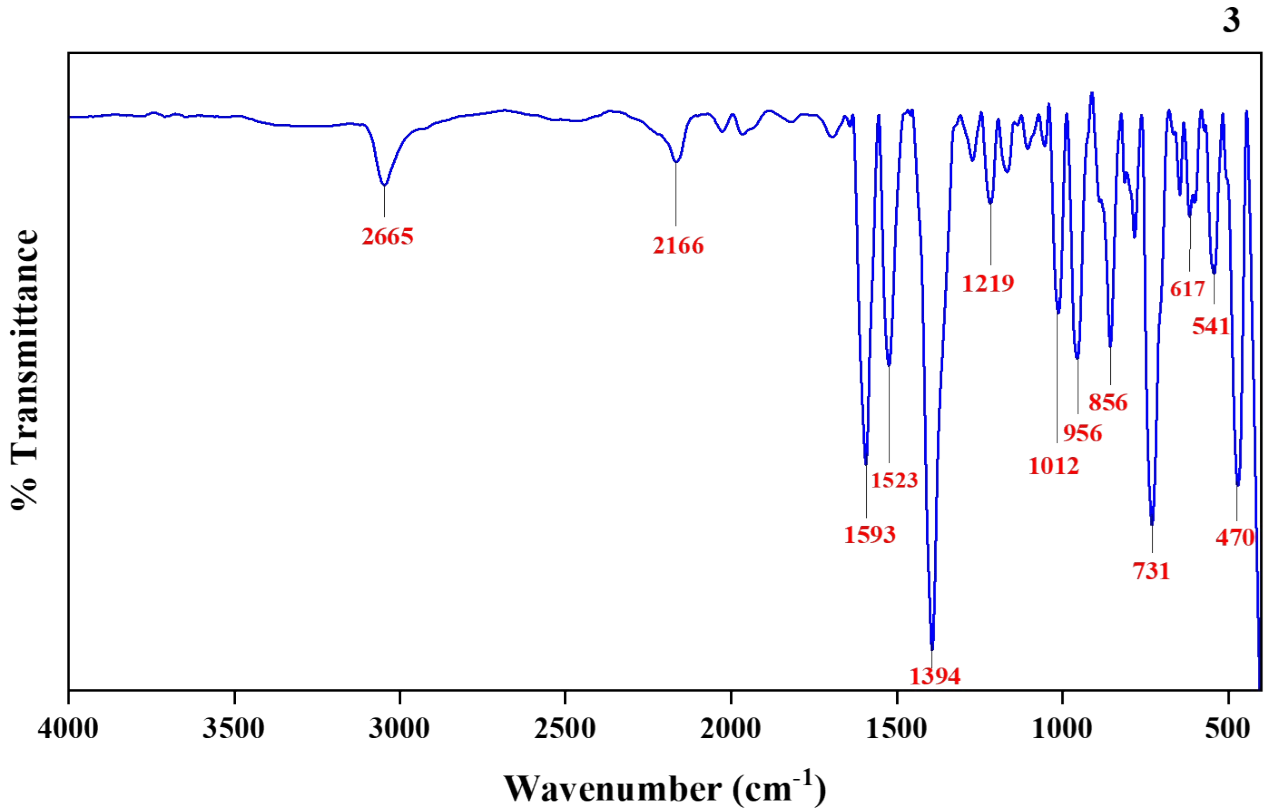

Fig. S34. FT-IR (KBr, cm^{-1}) spectrum of **3**.

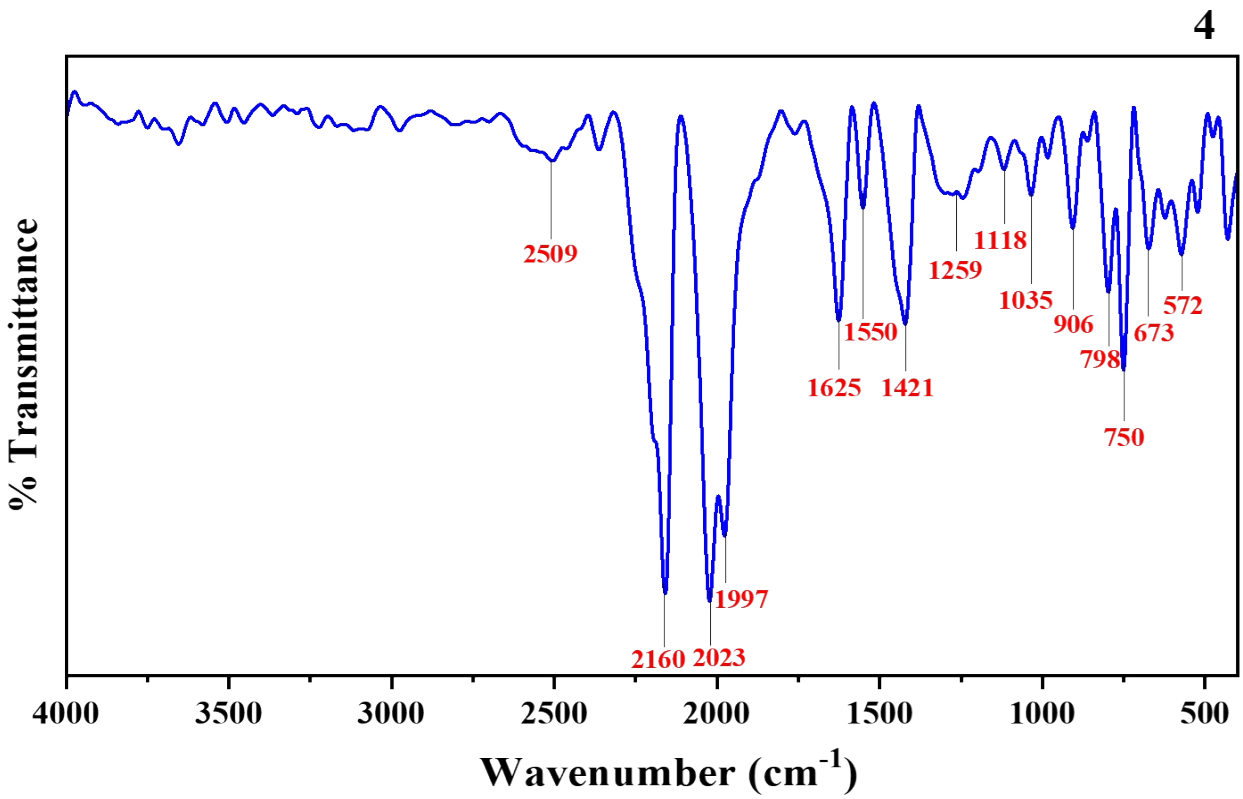

Fig. S35. FT-IR (KBr, cm^{-1}) spectrum of **4**.